ISSN: 2579-5821 (Print)
ISSN: 2579-5546 (Online)
URL address: http://journal.unhas.ac.id/index.php/geocelebes
DOI: 10.20956/geocelebes.v7i2.25371

Jurnal Geocelebes Vol. 7 No. 2, October 2023, 138 – 153

Middle Eocene Nannofossil Assemblages Responding to Depositional Dynamics of the Elat Formation, Maluku

Ratih C.F. Ratumanan[1*], Vijaya Isnaniawardhani[2*], Budi Muljana[3]

[1]Master Program in Geological Engineering, Padjadjaran University, 45363, Indonesia
[2,3]Department of Geosciences, Padjadjaran University, 45363, Indonesia

*Corresponding author. Email: ratihcfr@gmail.com, vijaya.isnania@unpad.ac.id

Manuscript received: 8 February 2023; Received in revised form: 6 June 2023; Accepted: 10 July 2023

Abstract

The Kei Besar Island is mainly composed of the Elat Formation carbonate rocks. This research was conducted to determine the nannofossils assemblages in the Elat Formation to interpret the depositional dynamics during its formation. Lithological observations and sampling for nannofossil analysis were carried out on three measured stratigraphic sections: Section 1 - Hollat, Section 2 - Ngurdu, and Section 3 - Mata Hollat. A total of 47 species assigned to 25 genera of nannofossils were identified in 45 selected samples. The succession of the Elat Formation in the study area formed at NP16 to N17 or Middle Eocene. Stratigraphic reconstruction supported by biostratigraphy analysis shows that Section 3 at the lower (NP16 to NP 17), Section 2 in the middle part (NP 17), and Section 1 at the upper (NP 17). R-mode cluster analysis of nannofossils defined four species clusters (assemblies A, B, C and D) that tend to occur together. Q-mode cluster analysis defined five depth-distribution clusters (1, 2, 3, 4, and 5), each deposited under similar conditions. Based on large foraminifera, the succession was formed in fore reef setting in neritic bathymetric zone. Coarsening and thickening upward supported by the nannofossil assemblages indicate depositional dynamics which tend to be shallower. Reworked fossils, commonly found at the lower of the Elat Formation, show the mechanism of turbid currents in early deposition.

Keywords: depositional environment; Kei Besar; Middle Eocene; nannofossil.

Citation: Ratumanan, R. C. F, Isnaniawardhani, V. and Muljana, B. (2023). Middle Eocene Nannofossil Assemblages as A Depositional Environment Indicator of Elat Formation, Maluku. *Jurnal Geocelebes*, 7(2):138–153, doi: 10.20956/geocelebes.v7i2.25371

Introduction

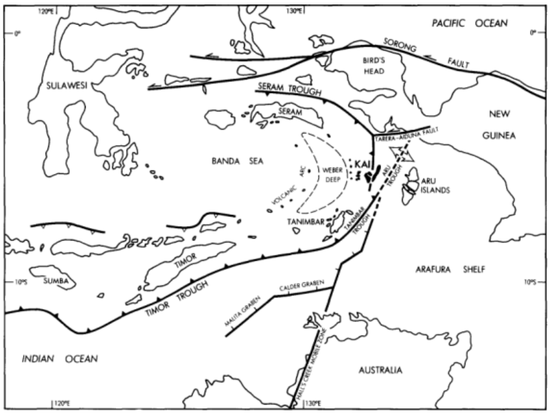

Figure 1. Kei Islands in the Banda Arc Tectonic Framework (modified from Charlton et al., 1991).

Geographically, the Kei Islands, Southeast Maluku, are in the arc zone of the Banda Arc System. The Banda Arc is located at the subduction zone between three plates in the earth's crust: the Indo-Australian Plate, the Eurasian Plate, and the Pacific Plate. The Banda Arc is divided into two regions, which are the Inner Banda Arc (volcanic) and the Outer Banda Arc (non-volcanic) (Charlton, 2016) (Figure 1).

The Kei Islands consist of Kei Besar Island and Kei Kecil Island. The Elat Formation occupies the most extensive area on Kei Besar Island. The Elat Formation is mainly composed of calcilutite and calcarenite, with marl intercalations. The thickness of this formation is estimated at 600 – 800 m. A thinning upward of marl indicates the depositional environment changes

(Achdan & Turkandi 1994). The Elat Formation refer as pelagic or hemipelagic carbonate rocks deposited on the distal continental slope setting, which is slowly shallowing. Based on the content of planktonic foraminifera, it is known that this formation was formed in the Middle to Late Eocene. Middle Eocene reworked benthic foraminifera fossils are found in calcilutite (Achdan and Turkandi, 1994; Charlton et al., 1991; Kurniasih et al., 2019).

Pelagic carbonate rocks as the Elat Formation usually contain many nannofossils (Agnini et al., 2017). These taxa are very small marine microfossils, oval, rod, star-shaped, nannofossil belongs to the protist kingdom, phylum hatophyta comporised of calcite plates generally produced by unicellular marine algal *coccolithophore* as a parent cell, limestone composisition, with a size of ±1-25 µm (Isnaniawardhani, 2017; Widhiyatmoko et al., 2023)

Nannofossil analysis provides good accuracy in determining relative ages of marine sediment because of the abundance, rapid evolution and wide distribution (Isnaniawardhani, 2015; Raffi et al., 2022). Quantitative analysis of nannofossils can be used to support the paleo-depositional environments, Paleotemperature and oceanographic reconstructions in addition to foraminifera (Isnaniawardhani et al., 2020; Karatsolis & Henderiks, 2023; Lowery et al., 2014; Choiriah & Maha, 2020; Villa et al., 2021; Imai et al., 2013; Rosmadi et al., 2022; Alves et al., 2016; Mandur et al., 2022).

The sampel of this research is the marine pelagic sediment of Elat Formation. This study focused on quantitatively analysing nannofossil assemblages, supported by lithostratigraphic data, to interpret changes in the depositional environment. The results of this study can then be used as a reference in reconstructing depositional environments based on nannofossil assemblages.

Materials and Methods

Field observations and sampling were carried out on 3 sections where the Elat Formation was continuously exposed. Five samples were collected from the northern part of Kei Besar Island (Section 1 or Hollat), 10 samples from the central part (Section 2 or Ngurdu), and 30 samples from the southern part (Section 3 or Mata Hola) (Figure 2). These samples were selected that contain assemblages of high-diversity nanofossils, and represent the upper, middle and lower stratigraphic positions of the formation.

Figure 2. Three sections of observation and sampling on Kei Besar Island, which are: Hollat (S-1), Ngurdu (S-2), and Mata Hollat (S-3)

The samples were prepared using the *quick smear slide method* (Suchéras-Marx et al., 2016; Young, 1998; Ikhwana et al., 2022; Farida et al., 2019). Observation of nannofossils was carried out using a polarizing microscope at 1000x magnification (Sheward., et al 2017; Gibbs et al., 2013). The determination of nannofossils refer to previous researchers such as Perch-Nielsen (1985), Young (1998), Nannotax3 (2014), Faris et al. (2021). Age determination is based on established biostratigraphy zones (Martini, 1971; Perch-Nielsen, 1985; Okada & Bukry, 1980; Agnini et al., 2014, Raffi et al., 2016).

Cascading counting method was applied in calculating the number of individuals of each species. The total abundance of individuals in the sample is classified into four classes (Ladner, 2007) (Table 1).

Table 1. Classification of individual abundance (Ladner, 2007).

Category	Number specimens per view
Abundant (A)	>10 per view
Common (C)	1-10 per view
Few (F)	1 specimen per 1-10 views
Rare (R)	< 1 specimen per 10 views

Diversity is calculated using the Shannon-Weaver index, as follows:

$$H' = -\Sigma\, p_i \, ln(p_i) \qquad (1)$$

where:

H' : Shannon-Weaver index

Σ : means "amount."

ln : natural logs

p_i : the proportion of the entire community consisting of species *i*

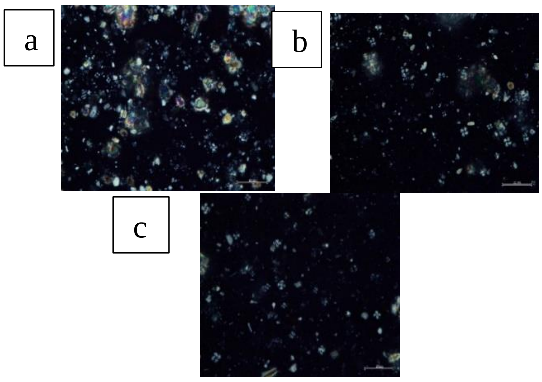

Figure 3. Photomicrograph of nannofossil preservation (a) Poor preservation (*Poor*) as shown in sample N4, (b) Medium preservation (*Fair*) on the sample MH16, (c) *Good* preservation on the sample MHL10

The data were processed using the *cluster analysis method* to compare the composition of taxa (*R-mode*) and the presence of distribution nannofossil assemblages in the sample (*Q-mode*) (Clark, 2018). The depositional environment is interpreted by integrating the results of the quantitative analysis to obtain accurate results (Kontakiotis et al., 2013). Preservation (Figure 3) of nannofossil was observed to provide an accurate interpretation (Roth, 1984) Preservation of nannofosil related to carbonate content in water-mass (Toffanin et al., 2013.), which were classification of preservation into three categories (Ladner, 2007) (Table 2).

Table 2. Classification of nannofossil preservation (Ladner, 2007).

Category	Description
Good (G)	little/no dissolution or *overgrowth*
Fair (F)	specimen shows some streaking and *overgrowth*
Poor (P)	specimen shows excessive streaking or *overgrowth*

Nannofossils cannot yet indicate depth in detail due to the nature of planktonic life. Therefore, large foraminifera analysis is also used for environmental (Hairul, 2022). Large foraminifera analysis was also carried out to strengthen the interpretation results. These fossils are founded in limestone intercalations. The determination of fossils refers to the systematic and occurrences of larger foraminifera.

Results and Discussion

Lithostratigraphy

The Elat Formation is composed of alternating calcarenite and calcareous clays, with limestone intercalations. Calcarenite is white-grey, fine to coarse sand, generally fine to medium in size, with parallel laminations, contains trace fossils, and thickness generally ranges from 5-70 cm. Towards the upper part, the grain size gets coarser, and the layer gets thicker, up to 1 meter. Fresh grey carbonate clay, weathered brownish, rich in fossils, poorly layered, generally <20 cm in thickness and decreases (<1 cm) upward. In several locations exposed white-brown limestone, containing large foraminifera and mollusk cells, generally < 10 cm thick (Figure 4–5, 8).

Stratigraphic reconstruction of the observation section based on the direction of the slope of the rock layers with a north-northeast trending trend and a gentle slope (< 50°). On section 3, the fold axis is found. The field observation indicates a depositional dynamic which tends to be shallower (Figure 6–7, 9).

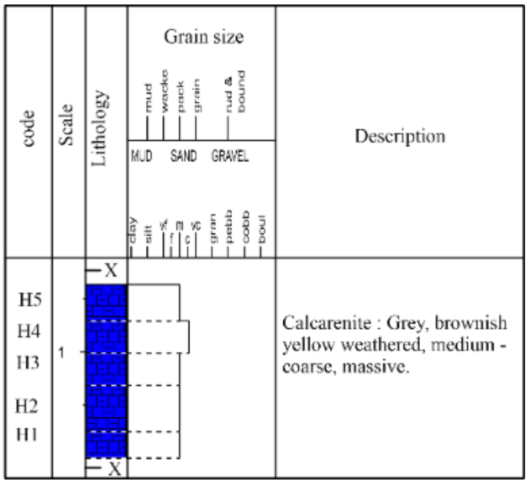

Figure 4. Lithostratigraphy S-1 Hollat.

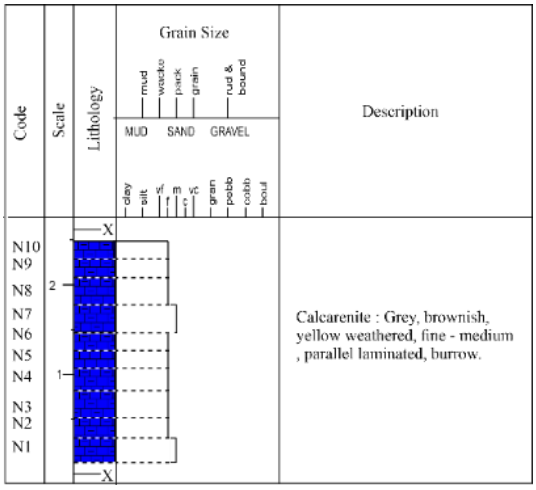

Figure 5. Lithostratigraphy S-2 Ngurdu.

Figure 6. Massive calcarenite on S-1 Hollat.

Figure 7. Calcarenite beds at S-2 Ngurdu.

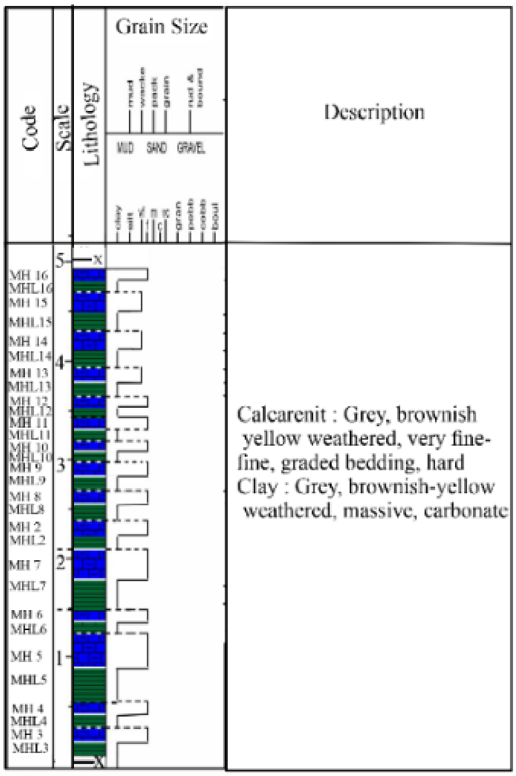

Figure 8. Lithostratigraphy S-3 Mata Hollat.

Figure 9. Intercalations of calcarenite and clay at S-3 Mata Hollat.

Table 3. Preservation, abundance, and individuals' number of nannofossil on S-1, -2, and -3.

Code	Preservation	Abundance	*Reticulofenestra umbilica*	*Reticulofenestra dictyoda*	*Reticulofenestrabisecta*	*Reticulofenestra stavensis*	*Reticulofenestra minuta*	*Reticulofenestra hampdanensis*	*Reticulofenestra lockeri*	*Cyligarcolithus floridanus*	*Cyclicargolithus luminis*	*Cocolithus pelagicus*	*Cocolithus aspida*	*Sphenolithus spiniger*	*Sphenolithus obtusus*	*Sphenolithus moriformis*	*Sphenolithus radians*	*Sphenolithus furcatholoides*	*Sphenolithus orphaknolensis*	*Helicosphaera compacta*	*Helicosphaera lopotha*	*Chiasmolithus grandis*	*Chiasmolithus titus*	*Chiasmolithus solitus*	*Umbilicosphaera protoannulus*	*Coronocyclus nitiscens*	*Clausicoccus subdistichus*	*Calcidiscus bicircus*	*Pontosphaera plana*	*Pontosphaera multipora*	*Pontosphaera pectinata*	*Pontosphaera wechesensis*	*Discoater kuepperi*	*Discoaster tani nodifer*	*Discoaster tanii*	*Braarudosphaera bigelowii*	*Scyphosphaera apsteini*	*Nanotetrina sp*	*Isthmolithus unipons*	*Ericsonia formosa*	*Zygrhablithus bijugatus*	*Lanterminuthus minutus*	*Isthmolithus sp*	*Blackites inflata*	*Tribrachiatus orthotylus*	*Rhabdosphaera gladius*	*Micrantholitus astrum*	*Faschitulithus tympaformis*	*Dictyococcites scripsae*
H5	F	C	2	9	5	0	1	1	0	7	2	4	0	6	4	2	7	5	1	4	4	0	0	0	0	0	0	1	0	0	0	0	0	0	0	4	0	0	0	5	5	2	0	0	0	0	0	0	0
H4	F	C	1	9	4	0	1	0	0	2	1	4	4	5	0	3	2	2	0	4	2	0	0	0	2	0	1	0	2	0	0	0	0	0	0	20	1	0	0	5	5	0	0	0	0	0	0	0	1
H3	F	C	2	11	4	0	1	1	0	7	2	3	1	5	1	3	4	1	1	3	4	1	0	0	0	0	2	0	0	0	0	0	0	2	0	9	0	0	0	4	3	0	0	0	0	0	1	0	1
H2	F	C	2	8	5	0	0	0	0	8	1	2	2	6	0	3	2	1	1	2	2	0	0	0	0	0	1	1	2	0	0	0	2	3	1	13	0	0	0	2	2	1	0	0	0	0	2	0	1
H1	G	C	0	9	4	0	2	0	0	7	1	5	0	5	0	2	3	3	0	4	0	1	0	0	0	0	0	0	0	0	0	0	0	0	0	20	0	0	0	4	3	0	0	0	0	0	0	0	0
N10	F	C	2	15	5	1	0	0	0	10	1	4	0	3	2	0	0	1	1	0	1	3	0	1	0	1	2	0	1	0	0	0	0	0	0	3	1	0	1	6	1	1	0	1	0	0	1	0	1
N9	G	C	4	22	10	0	8	3	1	19	1	2	0	4	1	1	0	1	1	2	0	3	0	1	1	0	0	0	1	0	0	0	0	3	0	2	0	0	0	4	1	1	0	0	0	0	0	0	1
N8	P	A	5	20	5	1	2	3	0	10	8	5	0	9	1	3	0	0	3	3	3	1	0	0	3	2	2	1	1	0	0	0	0	0	0	3	0	0	1	4	3	1	0	0	0	0	0	0	0
N7	P	C	2	13	7	2	5	1	0	10	1	8	0	3	2	3	1	0	1	4	0	0	1	0	1	2	1	0	2	0	0	0	0	0	0	3	1	2	0	5	2	0	0	0	0	0	2	0	2
N6	G	A	4	20	12	1	2	4	0	23	6	3	1	5	1	2	0	2	0	3	0	2	0	0	0	1	2	0	0	0	0	0	0	0	1	1	0	0	0	6	1	0	0	0	0	0	0	0	0
N5	F	A	7	15	5	0	1	0	0	26	3	7	0	9	0	7	0	0	3	0	1	1	1	1	2	1	3	0	0	0	0	0	0	0	0	3	0	0	0	10	2	0	0	0	0	0	0	0	0
N4	P	A	4	22	7	3	4	3	1	14	2	8	0	3	0	3	0	1	0	3	2	2	0	0	0	1	2	0	3	0	0	0	0	2	0	4	0	0	0	7	2	2	0	0	0	0	0	1	1
N3	G	C	7	21	10	1	4	3	0	15	1	10	0	4	0	4	0	0	0	2	2	0	0	0	0	2	0	0	0	0	0	1	0	0	0	3	0	0	0	6	3	1	0	0	0	0	0	0	2
N2	G	C	4	15	20	3	2	0	0	10	2	6	2	3	0	2	0	1	0	1	0	0	0	0	0	2	1	0	0	0	0	0	0	0	0	2	0	0	0	5	0	0	0	0	0	0	0	0	0
N1	F	C	4	16	10	5	1	4	0	11	4	6	1	5	0	4	0	0	1	2	0	0	0	0	0	2	3	1	2	0	0	0	0	0	1	5	0	0	0	7	2	1	0	0	0	1	0	0	1
MH16	F	A	12	26	10	4	0	1	0	35	2	8	1	8	0	4	0	0	2	1	1	0	0	1	3	4	2	0	2	0	1	1	0	1	2	2	0	0	0	9	0	8	0	0	1	0	0	0	0
MHL16	G	A	7	30	18	4	0	1	0	40	2	10	3	3	0	4	0	0	7	0	1	0	1	0	1	0	3	0	0	2	0	0	0	0	0	2	0	0	0	7	0	4	0	0	0	1	2	0	0
MH15	P	A	3	41	9	1	0	3	0	30	9	2	1	6	3	6	0	2	0	0	2	0	0	1	2	1	0	0	0	0	0	0	0	0	0	0	0	1	4	8	3	1	0	3	0	4	0	4	0
MHL15	G	A	5	35	4	8	0	0	0	24	4	10	0	7	1	0	0	2	2	1	2	0	0	2	1	3	4	1	4	1	0	0	0	2	3	2	1	0	7	10	1	9	0	1	2	1	1	0	0
MH14	F	C	1	30	11	3	0	0	0	20	2	5	0	4	1	1	2	2	2	1	0	0	0	0	7	5	0	4	3	0	0	0	0	2	0	0	1	0	2	3	3	5	0	2	0	0	0	6	0
MHL14	G	A	2	38	10	1	0	0	0	28	4	8	0	2	0	2	0	0	0	0	2	0	0	0	3	7	2	1	0	0	0	0	0	1	0	0	0	0	4	10	0	4	0	0	0	0	1	0	0
MH13	F	C	5	40	10	0	0	0	0	34	10	6	1	6	0	3	2	2	2	1	1	1	0	0	2	2	2	0	1	0	0	0	0	0	0	2	2	0	0	2	2	2	0	0	1	0	1	0	0
MHL13	G	A	4	50	18	3	0	0	0	42	1	12	0	4	0	1	1	0	2	0	3	0	0	0	0	2	4	2	0	0	0	0	0	2	0	1	0	0	0	10	0	4	0	0	0	0	1	0	0
MH12	F	C	3	23	6	3	0	2	3	19	4	6	1	2	0	2	0	0	1	0	2	1	0	0	1	0	1	0	0	0	0	0	0	1	0	2	0	0	0	3	1	1	0	0	0	0	0	0	0
MHL12	G	C	2	16	9	3	0	2	0	11	4	4	1	6	0	2	0	1	1	2	0	1	1	0	4	3	2	0	3	1	0	0	0	0	0	2	2	0	1	4	0	1	0	0	0	0	0	0	0
MH11	F	C	1	30	11	9	0	0	0	25	5	8	0	4	0	3	1	0	2	0	1	1	2	1	2	1	4	0	0	0	0	0	0	1	0	3	0	1	3	8	0	0	0	0	2	0	0	0	0
MHL11	F	A	10	32	15	2	0	0	0	21	6	17	0	8	0	2	0	2	1	2	2	0	0	1	1	16	2	0	1	0	0	0	0	2	0	0	0	2	1	8	0	4	0	0	0	1	1	0	0
MH10	G	C	2	22	9	1	0	0	0	14	4	6	0	6	0	2	1	0	1	0	0	1	0	0	0	1	0	0	2	0	0	0	0	1	0	0	0	0	0	9	11	0	0	1	0	0	0	0	0
MHL10	G	A	7	35	19	3	0	2	0	16	3	20	0	8	0	5	1	3	4	0	1	0	1	0	3	9	0	5	1	0	0	0	0	0	0	2	0	0	1	8	0	0	0	0	2	0	0	0	0
MH9	F	A	1	35	11	2	0	1	0	25	3	9	0	1	0	0	0	1	4	1	0	1	0	0	1	2	0	0	0	0	0	0	0	1	0	1	1	0	4	12	1	0	0	1	0	0	1	1	0
MHL9	G	A	10	33	15	3	2	2	0	28	6	15	0	9	0	4	0	3	2	1	1	1	1	0	0	5	9	2	3	0	0	0	0	0	0	1	0	0	0	8	6	0	0	0	0	0	0	0	0
MH8	F	C	9	24	10	3	0	0	0	9	4	18	0	2	0	1	0	0	5	1	1	0	1	0	3	3	3	1	1	1	0	0	0	0	0	0	0	0	2	12	0	5	0	0	0	1	0	0	0
MHL8	F	A	9	32	20	4	0	0	0	27	4	16	0	8	0	2	0	0	1	0	0	0	2	0	3	1	3	2	1	1	0	0	0	2	0	3	0	0	0	29	0	1	0	0	0	0	0	0	0
MH2	G	C	2	30	5	1	1	0	0	12	4	2	0	4	1	1	1	2	2	0	3	0	0	0	0	1	0	1	0	0	0	0	0	0	0	0	0	0	1	2	3	1	0	0	0	0	0	0	0
MHL2	G	C	7	70	10	3	2	3	0	21	0	17	0	0	1	0	0	1	0	0	0	0	0	0	3	1	3	0	0	0	0	0	0	0	0	1	1	0	0	11	0	0	0	0	0	0	0	0	0
MH7	G	C	2	35	12	2	2	0	0	21	4	5	1	9	0	1	0	0	0	0	1	0	0	2	0	0	0	2	3	0	0	0	0	0	0	1	0	0	3	5	1	2	0	0	0	0	0	0	0
MHL7	F	A	4	77	10	2	0	2	0	20	3	5	3	3	0	3	0	3	0	0	1	0	0	0	0	0	3	2	0	0	0	0	0	0	0	1	0	0	0	21	1	4	0	0	0	0	0	0	0
MH6	F	C	0	20	7	0	0	1	0	16	2	8	7	7	1	4	0	2	8	0	1	0	0	0	0	0	0	1	1	0	0	0	0	0	0	1	1	0	1	8	2	0	0	0	0	0	0	0	0
MHL6	F	A	0	40	12	0	0	0	0	15	9	23	0	18	0	0	0	0	3	0	2	0	0	0	7	1	0	0	3	0	0	0	0	0	0	0	0	0	5	14	2	4	2	0	0	0	0	0	0
MH5	P	C	0	49	13	0	0	0	0	26	4	3	0	8	2	4	0	0	0	0	3	0	0	0	0	0	0	0	1	0	0	0	0	0	0	0	0	0	0	3	2	0	1	0	0	1	0	0	0
MHL5	F	C	0	70	9	0	0	0	0	40	0	10	0	1	1	2	0	0	2	0	0	0	0	0	0	0	1	0	1	1	0	0	0	0	0	0	0	0	0	9	0	2	0	0	0	0	1	0	0
MH4	F	C	4	36	6	0	1	0	0	16	6	17	0	10	0	2	0	0	4	0	2	0	1	4	2	3	0	0	4	1	0	0	1	0	0	0	0	0	0	4	1	7	0	1	1	0	0	0	0
MHL4	G	C	1	32	11	2	0	1	0	25	5	10	0	4	0	4	0	0	3	0	4	0	0	1	0	0	0	0	0	2	0	0	0	0	0	1	0	0	0	8	0	2	0	1	0	0	0	0	0
MH3	F	A	7	30	12	8	0	0	0	15	5	4	0	8	0	2	0	3	7	0	1	0	7	6	1	0	1	0	2	0	0	0	0	0	0	0	6	3	3	15	1	3	0	0	0	0	0	0	0
MHL3	F	A	3	50	10	4	1	0	0	20	6	14	0	6	0	4	0	0	7	0	2	0	0	5	3	2	3	0	4	0	2	0	0	0	0	0	2	0	0	4	2	1	0	0	0	0	0	0	0

Nannofossil assemblages

In this study, nannofossil identified from the 45 selected samples were classified into 25 genera and 47 species (Table 3) in alphabetical order as follows:

- Genus *Blackites* (*B. inflata*)
- Genus *Braarudosphaera* (*B. bigelowii*)
- Genus *Calcidiscus* (*C. bicircus*),
- Genus *Chiasmolithus* (*C. grandis, C. solitus,* and *C. titus*)
- Genus *Clausicoccus* (*C. subdistichus*)
- Genus *Coccolithus* (*C. aspida,* and *C. pelagicus*)
- Genus *Coronocyclus* (C. *nitiscens*)
- Genus *Cyclicargolithus* (*C. floridanus,* and *C. luminis*)
- Genus *Dictyococcites* (*D. scrippsae)*
- Genus *Discoaster* (*D. kuepperi*, *D. tanii* and *D. tanii nodifier*)
- Genus *Ericsonia* (*E. formosa*)
- Genus *Fasciculithus* (*F. tympaniformis*)
- Genus *Helicosphaera* (*H. compacta*, and *H. lophota*)
- Genus *Isthmolithus* (*I. sp* and *I. unipons*)
- Genus *Lanternithus* (*L. minutus*)
- Genus *Micrantholithus* (*M. astrum*)
- Genus *Nanotetrina*
- Genus *Pontosphaera* (*P. multipora*, *P. pectinata*, *P. plana*, and *P. wechesensis*)
- Genus *Reticulofenestra* (*R. bisecta*, *R. dictyoda*, *R. hampdenensis*, *R. lockerii*, *R. minuta*, *R. stavensis*, and *R. umbilica*)
- Genus *Rhabdosphaera* (*R. gladius*)
- Genus *Scyphosphaera* (*S. apsteini*)
- Genus *Sphenolithus* (*S. furcatolithoides*, *S. moriformis*, *S. obtusus*, *S. orphaknolensis*, *S. radians*, and *S. spiniger*)
- Genus *Tribrachiatus* (*T. orthostylus*)
- Genus *Umbilicosphaera* (*U. protoannulus*)

- Genus *Zygrhablithus* (*Z. bijugatus*)

Biostratigraphy/ age identification

The marker species selected from the nannofossils assemblages were: *Reticulofenestra umbilica* and *Helicosphaera compacta.* Based on the presence of these species, the succession of the Middle Eocene Elat Formation can be grouped into two zones (Ratumanan, et al., 2022) (Table 4), which are:

a. *Reticulofenestra umbilica* Zone (NP16, or 43.06 to 38.7 million years ago)
b. *Helicosphaera compacta* Zone (NP17, 38.7 to 37.9 million years ago).

Rock succession on S-3 (southern part of Kei Besar Island) can be distinguished into the *Reticulofenstra umbilica Zone* (NP16) at the lower part, and the *Helicosphaera compacta* Zone (NP17) at the upper part. The all succession of Sections-1 and 2 includes the *Helicosphaera compacta* Zone (NP17).

This biostratigraphy analysis corelate to the stratigraphic reconstruction based on field data which shows the rocks are getting younger towards the north.

Table 4. Biostratigraphic zone on the three observation sections of the Elat Formation.

Sections	Epoch	Zone	Biozone
S-1 Hollat S-2 Ngurdu	Middle Eocene	NP17	Presence *Chiasmolithus grandis* (38.7 mya)
S-3 Mata Hollat			First appearance *Helicosphaera compacta* (37.9 mya)
		NP16	Appearance *Reticulofenestra umbilica* (43.06 mya)

Cluster Analysis

a. R-mode

For this cluster analysis, a similarity matrix was conducted based on relative abundance of species. This classification allows the characterization of four clusters (A, B, C, and D) which appear to coexist (Figure 10) of species that preferentially occur together.

Cluster A is characterized by an association of many placolith-bearing species (*Reticulofenestra umbilica, R. stavensis, R. minuta, R. hampdanensis, R. lockeri, Cyclicargolithus luminis, Cocolithus aspida, Helicosphaera compacta, H. lopotha, Chiasmolithus grandis, C. titus, C. solitus, Umbilicosphaera protoannulus, Coronocyclus nitiscens, Clausicoccus subdistichus, Calcidiscus bicircus, Pontosphaera plana, P. multipora, P. pectinate, P. wechesensis, Isthmolithus unipons, Ericsonia formosa, Isthmolithus* sp. , *Blackites inflata,* and *Dictyoccocites scripsae*), and *Sphenolithus obtusus, S. moriformis, S. radians, S. furcatholoides S. orphaknolensis, Discoater kuepperi, D. tani nodifer, D. tanii, Braarudosphaera bigelowii, Scyphosphaera apsteini, Nanotetrina* sp., *Zygrhablithus bijugatus, Lanterminuthus minutus, Tribrachiatus orthotylus Rhabdosphaera gladius, Micrantholitus astrum,* and *Faschitulithus tympaformis.*

Small placoliths are a good indicator of environmental conditions rich in nutrients in carbonate complexes (Okada, 2000; Aizawa et al., 2004) *Helicosphaera, Umbilicosphaera* and *Discoaster* are usually used to mark the neritic zone (Aizawa et al., 2004) The dominant *Discoaster* characterizes warm conditions (Pratiwi & Sato, 2016; Shepherd et al., 2021; D'Onofrio et al., 2021; Schneider et al., 2013). *Zygrhablithus bijugatus* indicated in low nutrient with open ocean envirotment (Gibbs et al., 2016; Fioroni et al., 2015), Reticulofenestra umbilica is temperate taxa (Bordiga et al., 2015; Senemari & Mejía-Molina, 2022). *Umbilicosphaera* is known as a tropical oligo taxon. *Braarudosphaera bigelowii* and *Reticulofenestra minuta* represent the photic zone species rich in nutrients (Kanungo & Young, 2017; Auer et al., 2014; Senemari & Jalili, 2021), The *Reticulofestra* group characterizes cold water (Umoh, 2023), *Chiasmolithus* is a characteristic of cold water (Khorassani et al., 2014; Kasem et al., 2022).

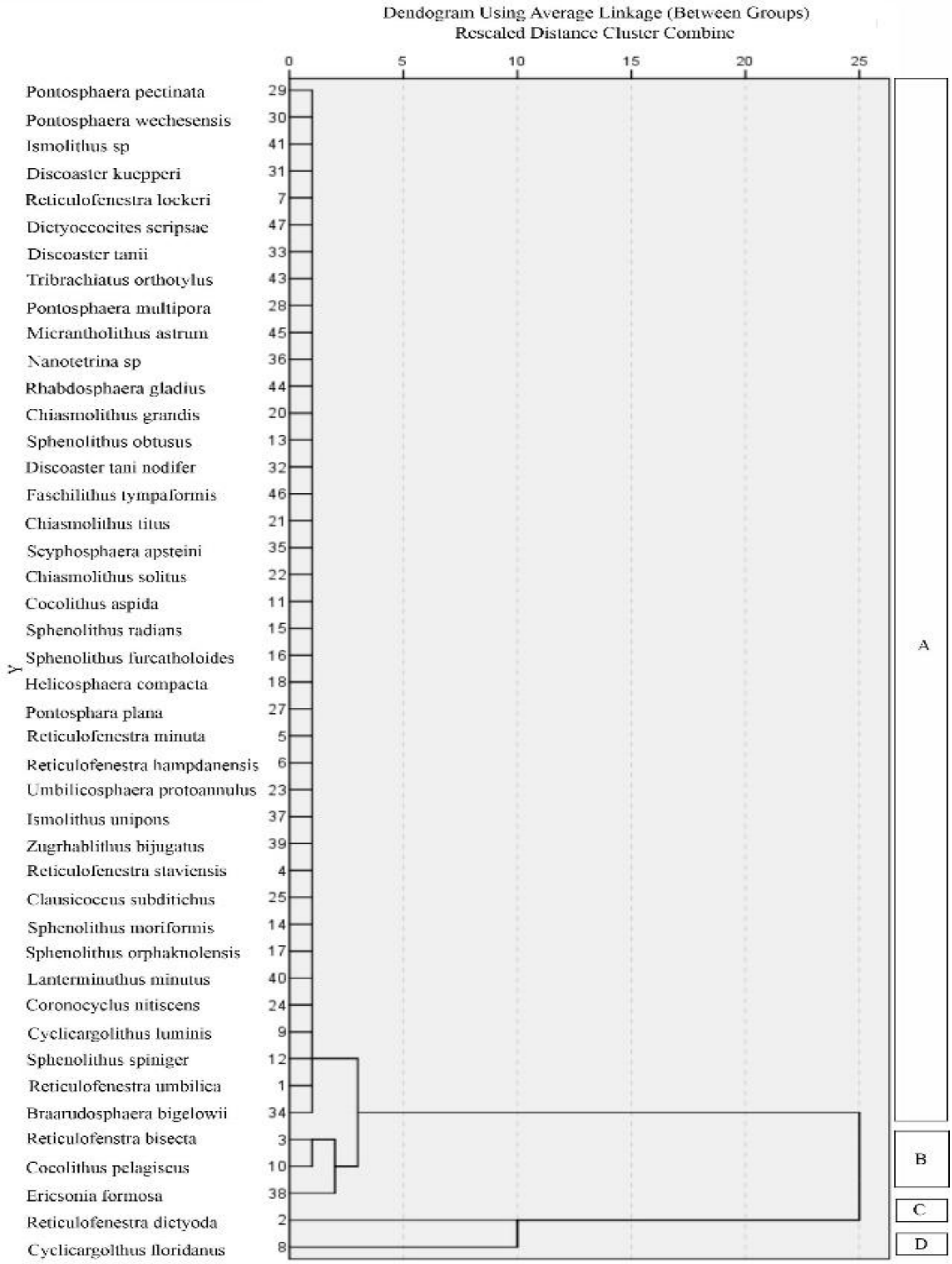

Figure 10. R-mode cluster analysis on three sections of the Elat Formation grouping into four clusters based on nannofossil associations (A, B, C, and D).

Cluster B represents the association *Ericsonia formosa*, *Reticulofenestra bisecta* and *Cocolithus pelagicus*. The dominant species, *Cocolithus pelagicus*, indicates cold water temperatures and represent in the upwelling zone (Kameo et al., 2020; Tangunan et al., 2018) .

Cluster C consists of a single species, which is *Reticulofenestra dictyoda.* Cluster D consists of the species *Cyclicargolithus floridanus* which characterize a high level of productivity (Monechi et al., 2000).

b. Q-mode

In this cluster analysis a similarity matrix is obtained based on the relative abundance of species from each sample. It has produced five clusters (1, 2, 3, 4, and 5) each of which represents the same environmental conditions (Figure 11).

Cluster 1 consists of all calcarenite samples from S-1 (sample codes H1 – H5) and S-2 (sample codes: N1 – N10), also five dominated calcarenite samples (MH6, MH8, MH10, MH12 and MHL12) from S-3. This cluster is characterized by the lowest abundance and diversity (abundance N= 70 to 120, average abundance Ń =91.9, and diversity index H' =2.88). This cluster has Poor (15%)-Good(40%) preservation with fair(45%) dominant.

Cluster 2 includes 11 calcarenite samples (MH2, MH3, MH4, MH5, MH7, MH9, MH11, MH13, MH14, MH15, and MH16), and 9 clay samples of clay (MHL3, MHL4, MHL6, MHL9, MHL10, MHL11, MHL14, MHL15, and MHL16) from Section-3 (N = 130-160, Ń = 144.4, and H' = 3.36). The clusters were poor (10,52%) - good (36,8%) preservation with a dominant fair preservation (52,6%) sample.

Cluster 3 is represented in one clay sample (MHL8) from Section-3 characterized by the highest abundance and diversity (N = 171, and H'=3.3). The cluster has a fair preservation and represented by this single sample are difficult to interpret.

Cluster 4 is represented by two clay samples, MHL2 and MHL7, from Section-3 which contain high abundance of nannofossil (N = 155-168, Ń = 161.5, and H ' = 2.5). The Clusters were good (50%) and fair (50%) preservation.

Cluster 5 includes two clay samples, MHL5 and MHL13, from Section-3 which contain high relative abundance (N=150-167, Ń= 158.5 and H ' =2.27). Cluster 5 were good (50%) and fair (50%) preservation

Large foraminifera assemblages

Large foraminifera identified from the limestone samples are genera *Amphistegina*, *Baculogypsina*, *Cycloclypeus*, *Heterostegina*, *Lacazinella Nummulites*, *Operculina*, *Pellatispira*, *Planobulinella* and *Textularia*. The observation showed the similarity of the large foraminifera assemblages at Sections-1, 2 and 3. Based on the assemblages, these lithological successions are formed at fore reef setting in neritic bathymetric zone (less than 200 meters depth).

Depositional Environment Dynamics

Stratigraphic reconstruction and biostratigraphy analysis show that the oldest rock succession from the Elat Formation is occupied by S-3 (aged NP16 to NP17), S-2 (aged NP17) in the middle, and the youngest is S-1 (aged NP17) (Table 5).

Nannofossil associated are dominated by placolith-bearing species, genus Discoaster, and *Braarudosphaera* that characterizes tropical warm-neritic (Newsam et al., 2017) taxa (Cluster A). Few cooler typical taxa were found in some samples (Cluster B).

Field observations recorded the coarsening and thickening upward of the lithological succession in the study area. Clay and alternating clay – calcarenite at the lower part (S-3) gradually changes to massive calcarenite at the upper part (S-1).

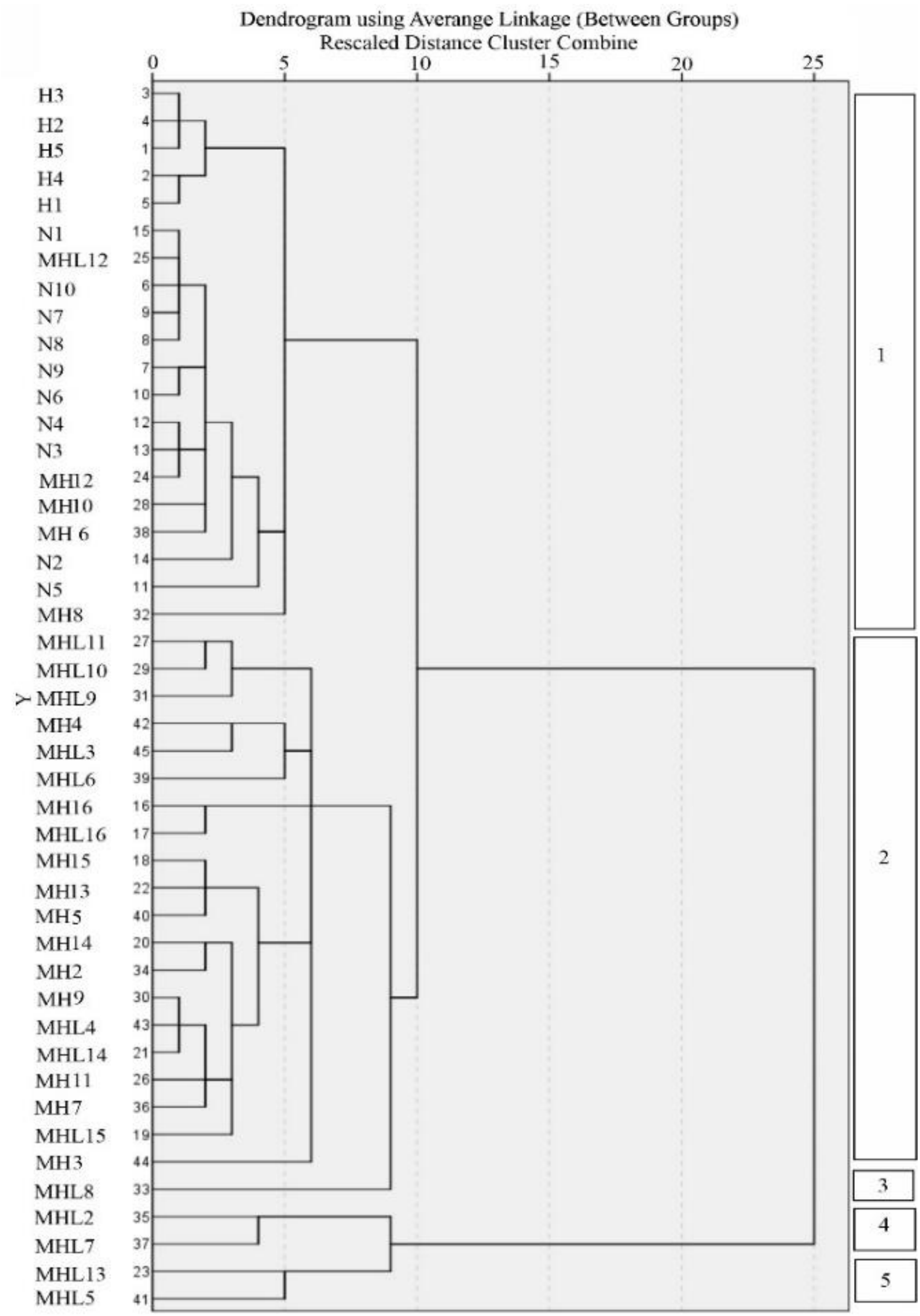

Figure 11. *Q-mode clusters* analysis on the three sections of the Elat Formation grouping into five clusters (1, 2, 3, 4, and 5) based on abundance.

Table 5. Depositional dynamics interpretation based on the assemblages of nannofossil recorded in the succession of the Elat Formation.

Section	Epoch	Age Zone	Code	Lithology	N	H'	C1	C2	C3	C4	C5
			H5	Calcarenite	81	2.87					
S-1			H4	Calcarenite	81	2.69					
Hollat			H3	Calcarenite	77	2.84					
			H2	Calcarenite	76	2.80					
			H1	Calcarenite	73	2.25					
			N10	Calcarenite	70	2.54					
		NP17	N9	Calcarenite	98	2.92					
			N8	Calcarenite	103	3.32					
			N7	Calcarenite	87	3.11					
S-2			N6	Calcarenite	103	2.92					
Ngurdu			N5	Calcarenite	108	2.98					
			N4	Calcarenite	107	3.40					
			N3	Calcarenite	102	2.98					
			N2	Calcarenite	81	2.38					
			N1	Calcarenite	100	3.29					
			MH16	Calcarenite	152	3.80					
			MHL16	Clay	153	3.39					
			MH15	Calcarenite	150	3.56					
	Middle		MHL15	Clay	161	4.33					
	Eocene		MH14	Calcarenite	128	3.60					
			MHL14	Clay	130	2.69					
			MH13	Calcarenite	143	3.29					
			MHL13	Clay	167	2.99					
			MH12	Calcarenite	88	2.61					
			MHL12	Clay	89	3.06					
			MH11	Calcarenite	129	3.34					
			MHL11	Clay	160	3.84					
			MH10	Calcarenite	94	2.60					
			MHL10	Clay	159	3.81					
S-3			MH9	Calcarenite	121	2.89					
Mata			MHL9	Clay	4.04	170					
Hollat			MH8	Calcarenite	3.32	120					
			MHL8	Clay	3.54	171					
			MH2	Calcarenite	2.31	80					
			MHL2	Clay	2.40	155					
			MH7	Calcarenite	2.80	114					
			MHL7	Clay	2.64	168					
			MH6	Calcarenite	99	2.84					
		NP16	MHL6	Clay	160	3.20					
			MH5	Calcarenite	120	2.15					
			MHL5	Clay	150	1.56					
			MH4	Calcarenite	134	3.39					
			MHL4	Clay	117	2.77					
			MH3	Calcarenite	150	3.40					
			MHL3	Clay	155	3.50					

The high abundance and diversity of nannofossil assemblages (Cluster 4 and 5) were shown at the lower part (S-3), while the lowest abundance and diversity (Cluster 1) at the upper part of the succession (S-1).

The abundance and diversity of nannofossils increases with increasing depth Changes in the composition of the nannofossil assemblages are consistent with changes in sediment grain size and lamination thickness indicating the dynamics of the depositional.

The presence of *Braarudosphaera* and *Reticulofenestra minuta* which are abundant in the middle to the upper part of the succession (on S-1 and -2) supports the interpretation that these rocks were formed in the neritic bathymetry zone. At the lower part (S-3) these taxa less indicate a deeper environment.

Observable depositional environment dynamics shallowing upward as recorded in field observations, supported by laboratory nannofossil assemblages, relevant to previous researchers (Achdan & Turkandi, 1994; Kurniasih et al., 2019) .

The similarity of the large foraminifera assemblages in all samples indicates that there was no significant bathymetric zone change during the Middle Eocene where lithological succession was formed. The dynamics of deposition occur in an inner neritic zone which tends to be shallower.

The presence of *reworked fossils* (*Blackites inflata, Cyclicargolithus luminis, Isthmolithus unipons, Nanotrina* sp., *Sphenolithus orphaknolensis, S. spiniger,* and *Tribrachiatus orthostylus*) which is dominant in S-3 can be interpreted due to turbid currents in the slope area that occurred at the beginning of the deposition of the Elat Formation. Field observations found local slump structures that support this interpretation.

Conclusion

The Elat Formation comprises fine-grained carbonate rocks containing abundant to very-very abundant nannofossils. A total of 47 species could be identified in the 45 selected samples from three sections (S-1 – Hollat, S-2 – Ngurdu and S-3 – Mata Hollat).

The succession of Elat Formation in study area was formed in NP16 to N17 or Middle Eocene. Reconstruction of lithostratigraphy and biostratigraphic analysis shows that the oldest rock succession from the Elat Formation is occupied by S-3 (aged NP16 to NP17), in the middle is occupied by S-2 (NP17), and the youngest is S-1 (NP17).

R-mode cluster analysis of samples grouped the nanofossil assemblages that appeared coexist into four clusters (A, B, C and D). *Q-mode* cluster analysis grouping into 5 clusters (1, 2, 3, 4, and 5) based on abundance and diversity which characterizes formation under the same environmental conditions.

Sediment grain size coarsening and lamination thickening are recorded in 3 sections. Changes in the composition of the nannofossil assemblages are consistent with lithological succession indicating depositional dynamics.

Reworked fossils at the lowermost of the Elat Formation (S-3) suggest a mechanism of deposition by turbidite currents.

Acknowledgements

Authors thank to Padjadjaran University for facilities support, and the Community of Kei Island for helping during field observation.

Author Contribution

Field observations were carried out by Ratumanan. Laboratory analysis was performed by Ratumanan and Isnaniawardhani. All authors discussed, interpreted, and wrote the manuscript.

Conflict of Interest

All authors have no any financial and personal relationships with other Community or organizations that could inappropriately influence (bias) our work.

References

Achdan, A., & Turkandi, T. (1994). *Peta Geologi Lembar Kai dan Tayandu, Maluku, Skala 1:250.000*. Pusat Penelitian dan Pengembangan

Geologi, Bandung.

Agnini C., Fornaciari E., Raffi, I., Catanzariti, R., Pälike, H., Backman, J., & Rio, D. (2014). Biozonation and biochronology of Paleogene calcareous nannofossils from low and middle latitudes. *Newsletter on Stratigrafi*, 47(2), 131–181. https://doi.org/10.1127/0078-0421/2014/0042

Agnini, C., Monechi, S., & Raffi, I. (2017). Calcareous nannofossil biostratigraphy: historical background and application in Cenozoic chronostratigraphy. *Lethaia*, 50(3), 447–463. https://doi.org/10.1111/let.12218

Aizawa, C., Oba, T., & Okada, H. (2004). Late Quaternary paleoceanography deduced from coccolith assemblages in a piston core recovered off the central Japan coast. *Marine Micropaleontology*, 52(1–4), 277–297. https://doi.org/10.1016/j.marmicro.2004.05.005

Alves, T. D., Cooper, M. K. E., & Rios-Netto, A. de M. (2016). Paleogene-Neogene calcareous nannofossil biostratigraphy and paleoecological inferences from northern Campos Basin, Brazil (well Campos-01). *Journal of South American Earth Sciences*, 71, 143–160. https://doi.org/10.1016/j.jsames.2016.06.010

Auer, G., Piller, W. E., & Harzhauser, M. (2014). High-resolution calcareous nannoplankton palaeoecology as a proxy for small-scale environmental changes in the Early Miocene. *Marine Micropaleontology*, 111, 53–65. https://doi.org/10.1016/j.marmicro.2014.06.005

Bordiga, M., Henderiks, J., Tori, F., Monechi, S., Fenero, R., Legarda-Lisarri, A., & Thomas, E. (2015). Microfossil evidence for trophic changes during the Eocene-Oligocene transition in the South Atlantic (ODP Site 1263, Walvis Ridge). *Climate of the Past*, 11(9), 1249–1270. https://doi.org/10.5194/cp-11-1249-2015

Charlton, T. R., Kaye, S. J., Samodra, H., & Sardjono. (1991). Geology of the Kai Islands: implications for the evolution of the Aru Trough and Weber Basin, Banda Arc, Indonesia. *Marine and Petroleum Geology*, 8(1), 62–69. https://doi.org/10.1016/0264-8172(91)90045-3

Charlton, T. R. (2016). *Neogene Plate Tectonic Evolution of The Banda Arc*. *Proceedings Indonesian Petroleum Association*. https://doi.org/10.29118/ipa.0.16.21.g

Choiriah, S. U., & Maha, M. (2020). *Aplikasi Nannoplankton untuk Interpretasi Paleotemperatur di Zona Kendeng*. Deepublish.

Clark, W. B. (2018). a Quantitative Analysis of Calcareous Nannofossils Across a Late Oligocene Paleolatiude Transect of the North Atlantic Ocean. *GSA Annual Meeting in Indianapolis, Indiana, USA*. https://doi.org/10.1130/abs/2018am-318571

Farida, M., Jaya, A., & Sato, T. (2019). Calcareous Nannofossil Assemblages of Tonasa Formation Palakka Area, South Sulawesi: Implication of Paleoenvironmental application. *IOP Conference Series: Materials Science and Engineering*, 619(1), 012016. https://doi.org/10.1088/1757-899X/619/1/012016

Fioroni, C., Villa, G., Persico, D., & Jovane, L. (2015). Middle Eocene-Lower Oligocene calcareous nannofossil biostratigraphy and paleoceanographic implications from Site 711 (equatorial Indian Ocean). *Marine Micropaleontology*, 118, 50–62. https://doi.org/10.1016/j.marmicro.2015.06.001

Gibbs, S. J., Bown, P. R., Ridgwell, A., Young, J. R., Poulton, A. J. & O'Dea,

S. A. (2016). Ocean warming not acidification controls coccolithophore response during past greenhouse climate change. *Geology*, 44(1), 59–62. https://doi.org/10.1130/G37273.1

Gibbs, S. J., Poulton, A. J., Bown, P. R., Daniels, C. J., Hopkins, J., Young, J. R., Jones, H. L., Thiemann, G. J., O'Dea, S. A., & Newsam, C. (2013). Species-specific growth response of coccolithophores to Palaeocene–Eocene environmental change. *Nature Geoscience*, 6, 218–222. https://doi.org/10.1038/ngeo1719

Hairul, N. S. (2022). *Biostratigrafi Formasi Tonasa Berdasarkan Nannofosil Daerah Mallasoro Kecamatan Bangkala Kabupaten Jenepont Provinsi Sulawesi Selatan*. Universitas Hasanuddin.

Ikhwana, N., Farida M., & Umar H. (2022). Paleoenvironment Analysis of the Tonasa Formation based on Nannofossils in the Barru River , South Sulawesi Province. *Proceedings PIT IAGI 51st*.

Imai, R., Sato, T., & Iryu, Y. (2013). Chronological and paleoceanographic constraints Miocene to Pliocene 'mud sea' in the Ryukyu Islands (southwestern Japan) based on calcareous nannofossil assemblages. *Island Arc*, 22(4), 522–537. https://doi.org/10.1111/iar.12046.

Isnaniawardhani V. (2015). *Biostratigraphy: Basics and Biostratigraphic Zones*. Universitas Padjadjaran, Penerbit Pustaka Reka Cipta.

Isnaniawardhani, V. (2017). *Prinsip dan Aplikasi Biostratigrafi*. UNPAD PRESS.

Isnaniawardhani, V., Rivaldy, M., Ismawan., Sophian, R. I., & Andyastiya, A. S. (2020). The Miocene (25.2 - 5.6 million years ago) climate changes recorded by foraminifera and nannofossils assemblages in Bogor Basin, Western Java. *IOP Conference Series: Earth and Environmental Science*, *575*(1), 012222. https://doi.org/10.1088/1755-1315/575/1/012222

Kameo, K., Kubota, Y., Haneda, Y., Suganuma, Y., & Okada, M. (2020). *Calcareous nannofossil biostratigraphy of the Lower–Middle Pleistocene boundary of the GSSP, Chiba composite section in the Kokumoto Formation, Kazusa Group, central Japan, and implications for seasurface environmental changes, Progress in Earth and Planetary Science*, 7, 36. https://doi.org/10.1186/s40645-020-00355-x

Kanungo, S., Young, J., & Skowron, G. (2017). Microfossils: Calcareous Nannoplankton (Nannofossils). In Sorkhabi, R., *Encyclopedia of Petroleum Geoscience*. Springer Link. https://doi.org/10.1007/978-3-319-02330-4

Karatsolis, B-T., & Henderiks, J. (2023). Late Neogene nannofossil assemblages as tracers of ocean circulation and paleoproductivity over the NW Australian shelf. *Climate of the Past*, 19(4), 765–786. https://doi.org/10.5194/cp-19-765-2023

Kasem, A. M., Faris, M., Jovane, L., Ads, T. A., Frontalini, F., & Zaky, A. S. (2022). Biostratigraphy and Paleoenvironmental Reconstruction at the Gebel Nezzazat (Central Sinai, Egypt): A Paleocene Record for the Southern Tethys. *Geosciences (Switzerland)*, 12(2), 96. https://doi.org/10.3390/geosciences12020096

Khorassani, M. P. K., & Hadavi, F., Ghasemi-Nejad, E., & Mousavi-Harami, R. (2014). Biostratigraphy and Paleoecological Study of Pabdeh Formation in Interior Fars, Zagros Basin, Iran. *Open Journal of Geology*, 4(11), 571–581.

https://doi.org/10.4236/ojg.2014.411042

Kontakiotis, G., Antonarakou, A., & Zachariasse, W. J. (2013). Late Quaternary palaeoenvironmental changes in the Aegean Sea: interrelations and interactions between North and South Aegean Sea. *Bulletin of the Geological Society of Greece*, 47(1), 167–177. https://doi.org/10.12681/bgsg.10920

Kurniasih, A., Qadaryati, N., & Setyawan, R. (2019). Surface geological investigation as the initial stage of hydrocarbon exploration in Kei Besar Island, Southern Maluku. *IOP Conference Series: Earth and Environmental Science*, 279(1), 012018. https://doi.org/10.1088/1755-1315/279/1/012018

Ladner, B. C. (2007). Data Report: Calcareous Albian, Nannofossil biostratigraphy of sediments recovered at site 1276, Ocean Drilling Program leg 210. In. Tucholke, B.E. Sibuet, J.-C., and Klaus, A. (Eds.). *Proc. ODP, Sci. Results, 210: College Station, TX (Ocean Drilling Program), 1–9.* http://www-odp.tamu.edu/publications/210_SR/113/113.htm

Lowery, C. M., Corbett, M. J., Leckie, R. M., Watkins, D., Miceli, R., & A., Pramudito, A. (2014). Foraminiferal and nannofossil paleoecology and paleoceanography of the Cenomanian-Turonian Eagle Ford Shale of southern Texas. *Palaeogeography, Palaeoclimatology, Palaeoecology*, *413*, 49–65. https://doi.org/10.1016/j.palaeo.2014.07.025

Martini, E. (1971). Standard Tertiary and Quaternary Calcareous Nannoplankton Zonation. *Proceeding of 2nd Conference Planktonic Microfossils, Rome (1970)*, 739–785.

Mandur, M. M. M., Hewaidy, A. G. A., Farouk, S., & El Agroudy, I. S. (2022). Implications of calcareous nannofossil biostratigraphy, biochronology, paleoecology, and sequence stratigraphy of the Paleocene-Eocene of the Wadi Qena, Egypt. *Journal of African Earth Sciences*, 193, 104594. https://doi.org/https://doi.org/10.1016/j.jafrearsci.2022.104594

Monechi, S., Buccianti, A., & Gardin, S. (2000). Biotic signals from nannoflora across the iridium anomaly in the upper Eocene of the Massignano section: Evidence from statistical analysis. *Marine Micropaleontology*, 39(1–4), 219–237. https://doi.org/10.1016/S0377-8398(00)00022-0

Faris, M., Farouk, S., & Shabaan, M. (2021). An overview of the Paleocene-Eocene calcareous nannofossil biostratigraphy and bioevents in Egypt. *Stratigraphy & Timescales*, 6, 225–292. https://doi.org/10.1016/bs.sats.2021.09.003

Nannotax3. (2014). *Nannotax 3*. https://www.mikrotax.org/Nannotax3/

Newsam, C., Bown, P. R., Wade, B. S., & Jones, H. L. (2017). Muted calcareous nannoplankton response at the Middle/Late eocene turnover event in the western North Atlantic Ocean. *Newsletters on Stratigraphy*, 50(3), 297–309. https://doi.org/10.1127/nos/2016/0306

Okada, H., & Bukry, D. (1980). Supplementary modification and introduction of code numbers to the low-latitude coccolith biostratigraphic zonation (Bukry, 1973; 1975). *Marine Micropaleontology*, 5, 321–325. https://doi.org/10.1016/0377-8398(80)90016-X

Okada, H. (2000). Neogene and Quaternary calcareous nannofossils from the Blake Ridge, Sites 994, 995, and 997. *Proceedings of the Ocean Drilling Program, Scientific Results,* 164, 331–341.

Perch-Nielsen, K. (1985). Cenozoic

Calcareous Nannofossils. in Bolli, H. M., Saunders, J. B., and Perch-Nielsen, K. (Eds.), *Plankton Stratigraphy*. Cambridge University Press, 427–554.

Pratiwi, S. D., & Sato, T. (2016). Reconstruction of Paleoceanography Significance in the Western Pacific and Atlantic Oceans during the Neogene Based on Calcareous Nannofossil Productivity and Size Variations, Related to the Global Tectonic Events. *Open Journal of Geology*, *06*(08), 931–943. https://doi.org/10.4236/ojg.2016.68070

Raffi, I., Agnini, C., Backman J., Catanzariti, R., & Pälike, H. (2016). Cenozoic calcareous nannofossil biozonation from low and middle latitudes: A synthesis. *Journal of Nannoplankton Research*, *36*(2), 121–32. https://doi.org/10.58998/jnr2206

Raffi, I., & Backman, J. (2022). The role of calcareous nannofossils in building age models for Cenozoic marine sediments : a review. *Rendiconti Lincei. Scienze Fisiche e Naturali*, *33*(1), 25–38. https://doi.org/10.1007/s12210-022-01048-x

Ratumanan, R. C. F., Isnaniawardhani, V., & Muljana, B. (2022). Nannofossil Biostratigraphy of Elat Formation, Kei Besar Island, Southeast Maluku. *IOP Conference Series: Earth and Environmental Science*., 1148(1), 012027. https://doi.org/10.1088/1755-1315/1148/1/012027

Rosmadi, N. S., Sulaiman, N., Sulaiman, N., & Asis, J. (2022). Biostratigraphy and paleodepositional environment of the Temburong Formation at Batu Luang, Klias Peninsula, Sabah based on calcareous nannofossil. *Journal of Tropical Resources and Sustainable Science*, *10*(1), 20–27. https://doi.org/10.47253/jtrss.v10i1.894

D'Onofrio, R., Zaky, A. S., Frontalini, F., Luciani, V., Catanzariti, R., Francescangeli, F., Giorgino, M., Coccioni, R., Özcan, E., & Jovane, L. (2021). Impact of the Middle Eocene Climatic Optimum (MECO) on Foraminiferal and Calcareous Nannofossil Assemblages in the Neo-Tethyan Baskil Section (Eastern Turkey): Paleoenvironmental and Paleoclimatic Reconstructions. *Applied Sciences*, 11(23), 11339. https://doi.org/10.3390/app112311339

Roth, P. H. (1984). Preservation of Calcareous Nannofossils and Fine-Grained Carbonate Particles in Mid-Cretaceous Sediments from the Southern Angola Basin, Site 530. *Deep Sea Drilling Project Reports and Publications*, 75, 651–655. https://doi.org/10.2973/dsdp.proc.75.112.1984

Schneider, L. J., Bralower, T. J., Kump, L. R., & Patzkowsky, M. E. (2013). Calcareous nannoplankton ecology and community change across the Paleocene-Eocene Thermal Maximum. *Paleobiology*, 39(4), 628–647. https://doi.org/10.1666/12050

Senemari, S., & Jalili, F. (2021). Eocene to Oligocene nannofossils stratigraphy and environmental conditions in Izeh Province, Zagros Basin, East Tethys. *Journal of Palaeogeography*, 10(10), 1–13. https://doi.org/10.1186/s42501-021-00092-2

Senemari, S., & Mejía-Molina, A. (2022). Calcareous nannofossil biostratigraphy and paleoenvironment of the Eocene–Oligocene interval in the Pabdeh Formation in southwestern Iran. *International Journal of Earth Sciences*, 111(4), 1289–1305. https://doi.org/10.1007/s00531-022-02180-7

Shepherd, C. L., Kulhanek, D. K., Hollis, C. J., Morgans, H. E. G., Strong, C. P., Pascher, K. M., & Zachos, J. C. (2021). Calcareous nannoplankton response to early Eocene warmth, Southwest

Pacific Ocean. *Marine Micropaleontology*, 165, 101992. https://doi.org/10.1016/j.marmicro.2021.101992

Sheward, R. M, Poulton, A. J., Gibbs, S. J., Daniels, C. J., & Bown, P. R. (2017). Physiology regulates the relationship between coccosphere geometry and growth phase in coccolithophores. *Biogeosciences*, 14, 1493–1509. https://doi.org/doi:10.5194/bg-14-1493-2017

Suchéras-Marx, B., Giraud, F., Lena, A., & Simionovici, A. (2016). Picking nannofossils: How and why. *Journal of Micropalaeontology*, 36, 219–221. https://doi.org/10.1144/10.1144jmpaleo2016-013

Tangunan, D. N., Baumann, K.-H., Just, J., LeVay, L. J., Barker, S., Brentegani, L., De Vleeschouwer, D., Hall, I. R., Hemming, S., Norris, R., & the Expedition 361 Shipboard Scientific Party. (2018). The last 1 million years of the extinct genus Discoaster: Plio-Pleistocene environment and productivity at Site U1476 (Mozambique Channel). *Palaeogeography. Palaeoclimatologu. Palaeoecology*, 505, 187–197. https://doi.org/10.1016/j.palaeo.2018.05.043

Toffanin, F., Agnini, C., Rio, D., Acton, G., & Westerhold, T. (2013). Middle Eocene to early Oligocene calcareous nannofossil biostratigraphy at IODP Site U1333 (equatorial Pacific). *Micropaleontology*, 59(1), 69–82. http://www.jstor.org/stable/24413317

Umoh, E. E. (2023). Palaeoecological Aspects of Nannoplankton Assemblages of AS-2 Well, Niger Delta. *Ajayi Crowther Journal of Pure and Applied Sciences*, 2(2). https://doi.org/10.556534/acjpas.2023.02.02.107

Villa, G., Florindo, F., Persico, D., Lurcock, P., de Martini, A. P., Jovane, L., & Fioroni, C. (2021). Integrated calcareous nannofossil and magnetostratigraphic record of ODP Site 709: Middle Eocene to late Oligocene paleoclimate and paleoceanography of the Equatorial Indian Ocean. *Marine Micropaleontology*, 169, 102051. https://doi.org/10.1016/j.marmicro.2021.102051

Widhiyatmoko, M., Isnaniawardhani, V., & Zajuli, M. H. H. (2023). Distribusi Nannofosil dan Foraminifera pada Batas Pliosen-Plistosen Formasi Batilembuti di Pulau Yamdena, Provinsi Maluku dan Relevansinya dengan Tektonik Regional. *Jurnal Geologi Dan Sumberdaya Mineral*, 24(1), 39–50. https://doi.org/10.33332/jgsm.geologi.v24i1.737

Young, J. R. (1998). *Calcareous Nannofosil Biostratigraphy* (P. R. Bown (ed.)). British Micropalaeontological Society Publications Series. Chapman & Hall. https://zarmesh.com/wp-content/uploads/2021/11/Calcareous-Nannofossil-Biostratigraphy.pdf